Solar Energy Materials & Solar Cells 121 (2014) 157–162

Contents lists available at ScienceDirect

Solar Energy Materials & Solar Cells

journal homepage: www.elsevier.com/locate/solmat

Stability of the regeneration of the boron–oxygen complex in silicon solar cells during module certification

Fabian Fertig *, Juliane Broisch, Daniel Biro, Stefan Rein

Fraunhofer Institute for Solar Energy Systems ISE, Heidenhofstr. 2, D-79110 Freiburg, Germany

ARTICLE INFO

Article history:
Received 8 August 2013
Received in revised form
16 October 2013
Accepted 17 October 2013
Available online 27 November 2013

Keywords:
Cz
Boron–oxygen
Module
Degradation
Regeneration

ABSTRACT

Light-induced degradation in boron-doped *p*-type Czochralski silicon is caused by a boron–oxygen complex, which may be permanently deactivated by simultaneous illumination and heating leading to a permanent regeneration of carrier lifetime and solar cell performance. To date, the long-term stability of the regenerated state under thermal stress has not been fully investigated. In this work, we investigate whether the regeneration gain achieved on solar cell level is stable upon accelerated aging tests such as thermal cycling and damp-heat testing as applied during module certification according to IEC and UL standards. It is shown that regeneration is mostly conserved upon thermal cycling and cells in the degraded state may even be regenerated if current is injected during the treatment. Damp-heat testing at 85 °C in the dark for 1500 h decreases the regeneration-induced gain significantly but does not annihilate it completely.

1. Introduction

One of the most widely used sources for solar silicon (Si) wafers are boron-doped monocrystalline silicon ingots crystallized via the Czochralski (Cz) technique [1,2]. During Cz crystallisation, oxygen diffuses from the walls of the quartz crucible into the silicon melt and is incorporated into the silicon crystal [1,2]. Along with boron, oxygen can form the highly recombination-active boron–oxygen (BO) defect [3,4] which, in its active state, limits the excess carrier lifetime in industrial Cz *p*-type silicon significantly and therefore the maximum conversion efficiency of *p*-type silicon solar cells [5,6]. Extensive research work in the past revealed that the defect is metastable and can be activated upon illumination or carrier injection and fully deactivated upon annealing in the dark [7,8], the transformation between the two defect states being fully reversible.

More recently, Herguth et al. [9] found a methodology to permanently deactivate the BO defect by combined carrier injection and annealing, which is known as regeneration. Reported temperatures required for regeneration vary from $T=70$ °C to 215 °C [9,10] with $T=140$ °C usually not being exceeded for the regeneration of solar cells (in contrast to lifetime samples). Destruction of the regenerated state and therefore reactivation of the defect may occur at elevated temperatures of $T>170$ °C in the dark [9] and after illumination at elevated temperatures for a long time [10,11] while the latter effect is not always observed [11].

We have shown, that the regeneration of the BO defect within passivated emitter and rear (PERC) solar cells on cell level is stable upon module assembly including soldering and lamination [12]. However, no information is available on the stability of the regenerated state during continued module operation. To simulate worst case operating conditions on a comparatively short time-scale, accelerated aging tests are performed during module certification [13,14]. Hence, this work aims at investigating the stability of the regenerated state of the BO defect upon selected accelerated aging tests as performed during module certification to check whether the achieved performance gain due to regeneration on cell level can be conserved during worst case module operating conditions.

2. Experimental

The stability of the BO complex' regenerated state is evaluated on PERC solar cells [15] fabricated on industrial equipment at Fraunhofer ISE [16]. The cells feature a thin thermal oxide for passivation, stacked with a silicon nitride anti-reflective coating on the front and a dielectric layer on the rear, screen-printed metallisation, laser fired contacts [17] and a laser doped selective emitter. Details on cell structure and applied cell process can be found in Refs. [18,19]. Industrial, boron-doped *p*-type Cz Si wafers[1] with a base resistivity of $\rho_{b,Cz}=2.3\ \Omega$ cm and FZ Si wafers with $\rho_{b,FZ}=0.5\ \Omega$ cm are processed equally within the same batch.

* Corresponding author. Tel.: +49 761 4588 5482.
E-mail address: fabian.fertig@ise.fraunhofer.de (F. Fertig).

[1] Area 148.58 cm^2, thickness 200 μm before / 160 μm after cell processing.

0927-0248/$ - see front matter © 2013 Elsevier B.V. All rights reserved.
http://dx.doi.org/10.1016/j.solmat.2013.10.014

The FZ wafers serve as a reference to monitor possible process-induced effects through the subsequent treatment after cell processing which are not material-related.

Two very similar Cz solar cells (cells A/B) and one FZ reference cell are subjected to the treatment depicted in Fig. 1. In-between each experimental step, all cells respectively modules are characterised by means of *I–V* (current–voltage) and suns–V_{oc} [20] measurements. To avoid any possible impact of stray radiation, the cells respectively modules are kept in the dark in-between experimental step and conducted measurements. Cell and module measurements are performed using the same flash lamp.

Before module integration, Cz cell A is conditioned in the degraded and Cz cell B in the regenerated state. The FZ cell is treated equally as Cz cell B. The applied parameters are given in Fig. 1 and are discussed in detail in Ref. [12] up to thermal cycling.

Thermal cycling (TC) and damp heat (DH) testing are performed in dark, temperature- and humidity-controlled climate chambers at Fraunhofer ISE TestLab PV Modules.

2.1. Thermal cycling

During the first run, 95 cycles between $T_{low}=-40$ °C and $T_{high}=85$ °C are conducted with a cycle time of $t=4$ h. Fig. 2 depicts the temperature profile measured on a reference module. For $T>25$ °C, a current of $I=5\ \text{A}\approx I_{MPP}$ is injected which is reduced to $I=0.25$ A for $T<25$ °C. This procedure correlates to the "TC200 test" (200 cycles) within certification standard IEC-61215 [13]. Subsequently, the modules are illuminated to check if the defect is still in its regenerated state. The second run includes the same temperature ramps as run 1, see Fig. 2, but for 200 cycles without current injection. The temperature profiles of run 1 and 2 slightly differ because different chambers with differing heat capacities have been used. This test correlates to the "TC50 test" (50 cycles) in IEC-61215 and the "TC test" (200 cycles) in standard UL-1703 [14]. Afterwards, the modules are illuminated again to check for the stability of the regenerated state.

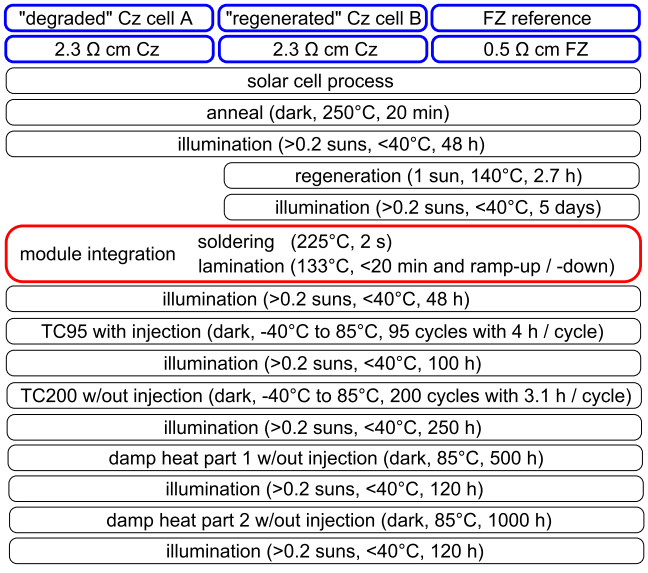

Fig. 1. Sketch of the experimental design. Before module assembly, Cz cell A is in the "degraded" state, while Cz cell B and a FZ reference cell are in the "regenerated" state. In-between each step, *I–V* and suns–V_{oc} measurements are performed.

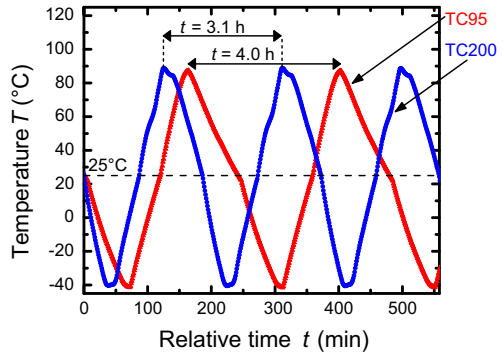

Fig. 2. Cut-out of the temperature profiles measured on a reference module during thermal cycling tests.

2.2. Damp heat

Both addressed standards include a "humidity (freeze) test" which includes 10 cycles in-between $T_{low}=-40$ °C and $T_{high}=85$ °C at a humidity of 85% with $t(T_{high})\geq 20$ h per cycle. Within the IEC standard, an additional "damp-heat" test is performed maintaining $T_{high}=85$ °C for $t=1000$ h at the same conditions as during "humidity freeze". Within our experiment, see Fig. 1, we first performed damp-heat testing for $t=500$ h without current injection and subsequently illuminated the modules. Then, damp heat is repeated for $t=1000$ h, again without current injection, followed by illumination of the modules.

3. Results

Fig. 3 summarizes the results of the *I–V* and suns–V_{oc} measurements[2] after each experimental step. Fig. 3a depicts absolute measured values and Fig. 3b–d the absolute differences in V_{oc} and *pFF* with respect to different reference points. Those are for Fig. 3b all cells "after moduling" and for Fig. 3c all cells "degraded on cell level". Fig. 3d displays the values of the Cz cells with respect to the values of the FZ reference cell in each step.

3.1. Before thermal cycling

Comparing the annealed to the degraded state of the BO defect prior to moduling, Cz cells A/B degrade in maximum output power by $\Delta P_{MPP}=-0.13/-0.12$ W which correlates to an efficiency loss of $\Delta\eta=-0.9/-0.8\%_{abs}$. This loss is composed of a loss in all illuminated *I–V* parameters. The change in fill factor *FF* is mainly due to a loss in pseudo fill factor *pFF* which is caused by a change in the injection dependence of the bulk lifetime upon defect activation [12,21]. For Cz cell B, the losses can almost be completely recovered by regeneration and are stable upon subsequent illumination. The FZ cell is treated equally to Cz cell B showing no significant degradation.

Upon module assembly and subsequent illumination, open-circuit voltage V_{oc} and *pFF* are maintained while *FF* equally degrades for all cells due to additional series resistance in the cell interconnectors and feed lines. The short-circuit current loss ΔI_{sc} of Cz cell A is slightly lower compared to the other two cells, which is most likely due to differing optical coupling [12]. However, compared to the FZ reference cell, the gain in all illuminated *I–V* parameters due to regeneration on cell level can be transferred to module level. All results up to TC are thoroughly discussed in Ref. [12].

To visualize the effect of the injection-dependent bulk lifetime of the BO defect on solar cell performance, we subtract the suns–V_{oc} characteristics in each step from the one measured in the annealed state for each cell. Fig. 4 shows the difference in V_{oc}

[2] To control the effect of total internal reflection under the module glass, all module measurements have been recorded using a square shading pattern with an opening of $A=127\times 127$ mm^2 simulating the symmetry element in an industrial module with a distance of the cells of $d=2$ mm.

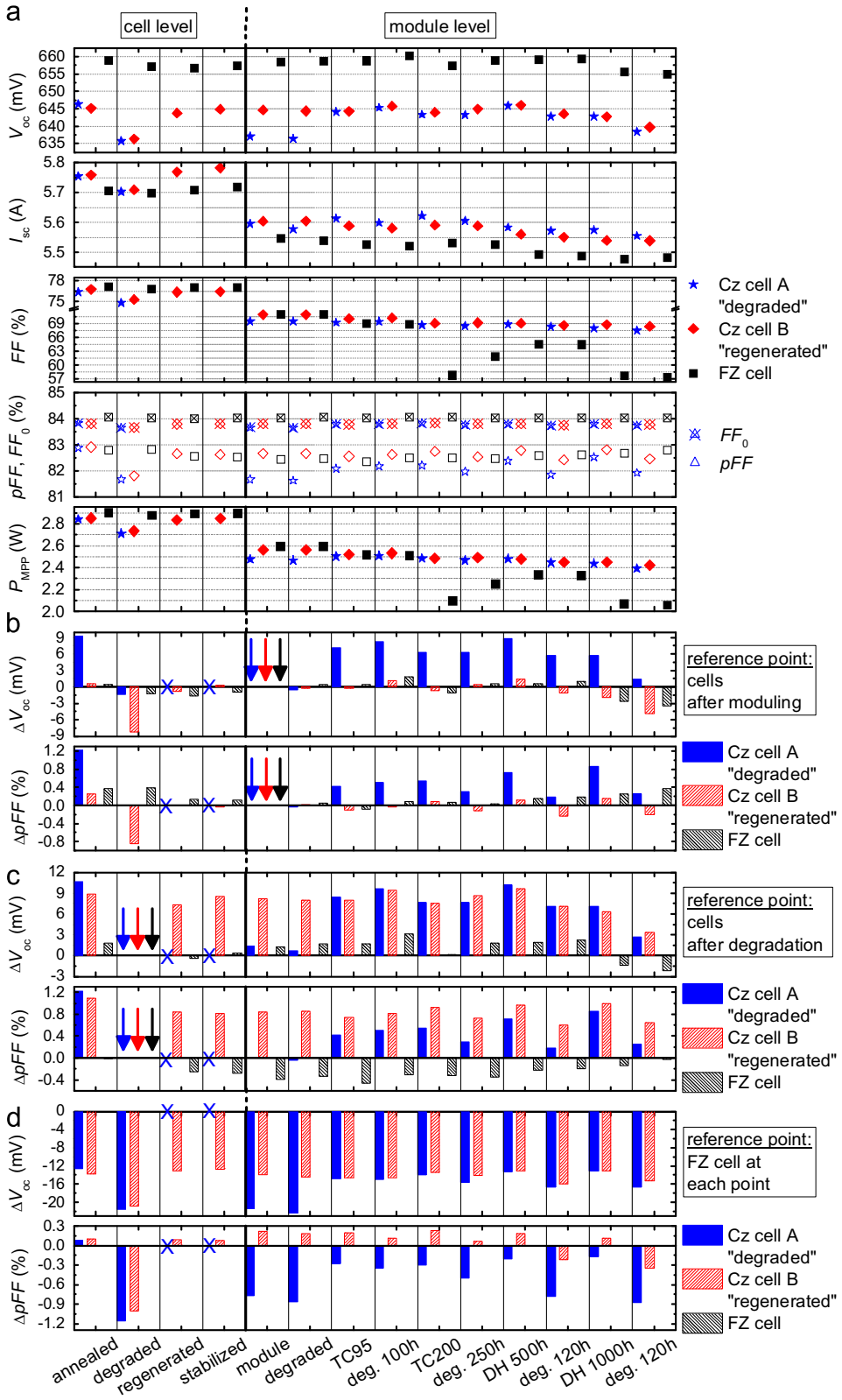

Fig. 3. **(a)** Measured illuminated *I–V* parameters open-circuit voltage V_{oc}, short-circuit current I_{sc}, fill factor *FF*, pseudo fill factor *pFF*, ideal fill factor FF_0 (according to Green, p. 96 in [26]), and maximum output power P_{MPP} after each conditioning step sketched in Fig. 1 for two Cz cells conditioned in different defect states prior to module fabrication and one FZ cell as a reference. **(b)** Absolute differences in the different conditioning steps compared to values **after module integration** (indicated by arrows) for each of the three cells. **(c)** As (b) compared to values **after degradation on cell level. (d)** As (b) and (c) compared to the values of the FZ reference cell in each step.

for varying illumination intensity E and therefore injection level Δn. When for example considering the degraded state of Cz cell A, it can be seen that $\Delta V_{oc}(E=0.05\ \text{suns})=17$ mV at the pseudo maximum power point (pMPP) is significantly higher than $\Delta V_{oc}(E=1.0\ \text{sun})=11$ mV under one-sun conditions as applied during the *I–V* measurement, compare Fig. 3. This difference in

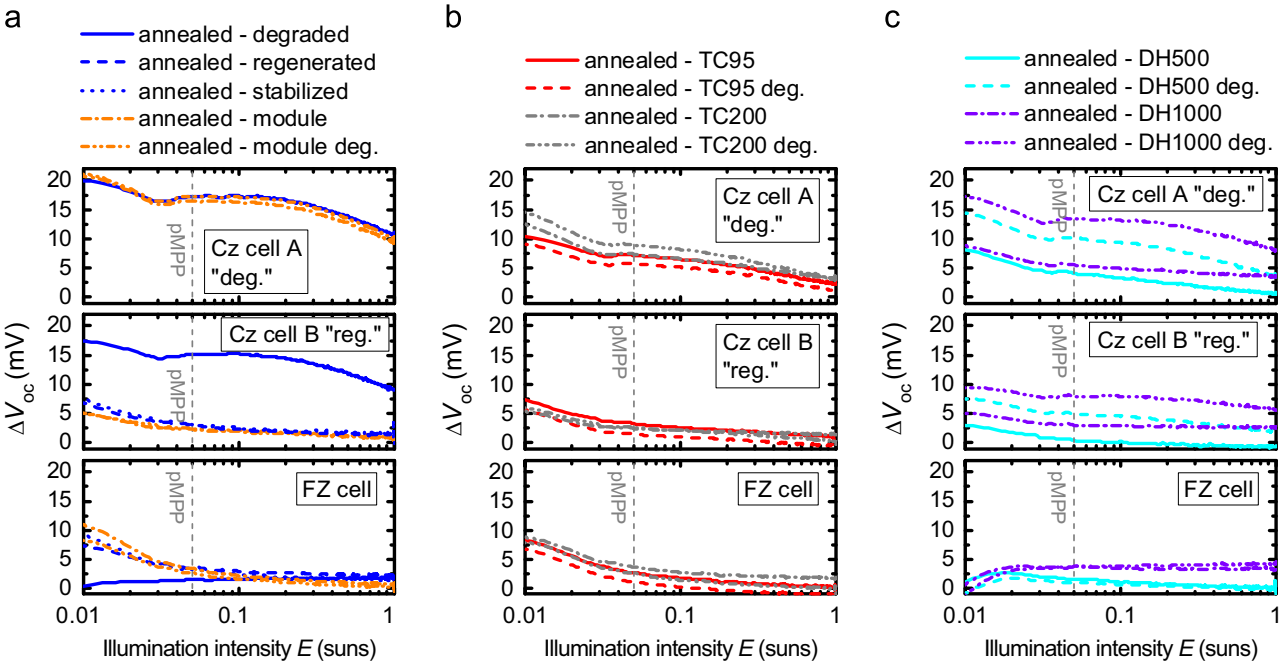

Fig. 4. Difference in open-circuit voltages V_{oc} in-between the different defect states and the annealed state for the three cells as a function of illumination intensity E. Data have been recorded via suns–V_{oc} measurements. **(a)** Cell and module level prior to certification testing. **(b)** Thermal cycling. **(c)** Damp heat.

ΔV_{oc} for varying injection level is the root cause for the pseudo fill factor degradation of $\Delta pFF = -1.2\%_{abs}$ in-between the annealed and degraded state of Cz cell A, see Fig. 3c. A detailed theoretical motivation for the depicted analysis is given in Ref. [12].

Fig. 4a shows that the injection dependencies of ΔV_{oc} do not change significantly for all cells upon module integration and subsequent illumination indicating no change in the state of the BO defect. The further discussion focuses on V_{oc} and pFF unless explicitly mentioned. All parameters are given in Figs. 3 and 4.

3.2. Thermal cycling

Cz cell B and the FZ reference cell show no significant degradation in their illuminated I–V parameters during the TC95 test (with current injection) and subsequent illumination. Also, the injection dependence of ΔV_{oc} does not change significantly, see Fig. 4b, which indicates that Cz cell B is still in the regenerated state. For Cz cell A, V_{oc} and pFF increase by $\Delta V_{oc} \approx 8$ mV and $\Delta pFF \approx 0.5\%_{abs}$ upon TC95. This partly compensates the degradation-induced loss on cell level of $\Delta V_{oc} = -11$ mV and $\Delta pFF = -1.0\%_{abs}$. Since Cz cell A is stable upon subsequent illumination, the BO defect seems to be partly regenerated. This conclusion is supported by the change in injection dependence of ΔV_{oc} upon TC95 testing, see Fig. 4b. The difference to the annealed state is significantly less pronounced than for Cz cell A being in the degraded state, compare Fig. 4a. However, the injection dependence is not reduced to the same level as for Cz cell B in the regenerated state, see Fig. 4b.

It is known [22] that regeneration cannot only be induced by illumination but also by carrier injection in the dark at elevated temperatures. For a rough estimate of theoretical regeneration times, we extrapolated Herguth's data on the regeneration time constant for V_{oc}, which is determined for a temperature range of $T = 100$ °C to 140 °C in Ref. [9], to the temperature range of $T = -40$ °C to 85 °C as applied during TC. For the regeneration process applied on cell level during this work, we extracted a regeneration time constant of $1/\tau_0(T = 140\ °C) \approx 5 \times 10^{-2}\ min^{-1}$. The constant was determined by fitting an exponential function to time-dependent measurement data of V_{oc} during regeneration. Since this extracted value is about half of Herguth's value[3] for $T = 140$ °C, we divided the resulting regeneration time constants from the performed extrapolation by a factor of 2. Assuming a constant factor for the correction represents a rough estimate since it has been shown [23] that the extracted activation energy for the regeneration process depends on the boron concentration of a Cz silicon wafer. Using this extrapolation, 98% of regeneration is expected to occur within the applied temperature treatment during TC95 shown in Fig. 2. However, the injection level at I_{MPP} in the dark is lower than under V_{oc} at 1 sun illumination [12], which could explain a slower regeneration process. That lower injection levels at constant temperature can lead to a slower regeneration rate has been shown before [24]. In summary, although the available data on the kinetics of the regeneration process are limited, significant regeneration during TC95 with current injection can be expected which is confirmed by the experimental data.

After TC200 (without current injection) and subsequent illumination, none of the cells degrade dramatically in V_{oc} and pFF. By extrapolating Herguth's data [9] on the destabilization of the regenerated state in the dark (data are given for the temperature range of $T = 170$ °C to 200 °C), 10% (that is $\Delta V_{oc} \approx 1$ mV) of the regeneration-induced gain is predicted to be lost during TC200. To the knowledge of the authors, for the destabilization process neither the dependence of the destabilization rate nor the activation energy on boron or oxygen concentration has been investigated to date. Hence, the performed extrapolation, again, represents a rough estimate. However, it suggests that due to the limited number of samples a destabilization-induced loss in the order of 1 mV will be difficult to be verified experimentally. When comparing the changes of V_{oc} and pFF of the Cz cells compared to the FZ cell after TC200 and after the subsequent illumination step, see Fig. 3d, a slight loss of $\Delta V_{oc} \approx -1$ mV and $\Delta pFF \approx -0.2\%_{abs}$ can

[3] Possible reasons can be different boron and/or oxygen concentrations in the Cz wafers and/or different injection conditions during regeneration.

be observed. Also, a slight increase in injection dependence of ΔV_{oc} before and after illumination compared to the annealed state is indicated by suns–V_{oc} measurements, see Fig. 4b. Compared to the FZ cell, a loss of $\Delta V_{oc}(E=0.05\ \text{suns}) \approx -3/-2$ mV is measured for Cz cells A/B.

Due to the very limited statistics, these little variations need to be interpreted with care. Interpretation (i) for the observed trends could be partial annealing of the non-regenerated share of the defect during TC200 without a change in concentration of the regenerated state. This interpretation is supported by the increase in injection dependence upon illumination after TC200 seeming to be slightly higher for Cz cell A (defect partly regenerated) compared to Cz cell B (defect almost completely regenerated), see Fig. 4b. Also, the degradation upon illumination in V_{oc} and *pFF* compared to the FZ cell is slightly higher for Cz cell A than B, see Fig. 3d. Since in literature [9], for the destabilization of the regenerated state, its transformation into the annealed state prior to light-induced re-degradation is suspected, interpretation (ii) would be a small amount of destabilization of the regenerated state in both Cz cells A and B during TC200. This interpretation would be supported by the observation that both Cz cells degrade in V_{oc} and *pFF* compared to the FZ reference cell, see Fig. 3d. That Cz cell A seems to degrade a little more than Cz cell B indicates that both interpretations could contribute to the observed effects. However, it is stressed again that this interpretation needs to be considered with care due to the small observed variations and the very limited statistics.

For all three cells, *FF* decreases during TC which can be caused by degradation of the leads. For the FZ cell, series resistance imaging [25] indicates a significant deterioration of the contact resistance of one busbar during TC200 which leads to the stronger decrease in *FF*. However, *pFF* is not significantly affected. Concerning I_{sc}, Cz cell A shows a significant increase due to the observed regeneration. Compared to the FZ cell, an increase of $\Delta I_{sc}=49$ mA is observed during TC95 which is in the same order as the regeneration-induced increase of $\Delta I_{sc}=51$ mA for Cz cell B on cell level.

In summary, Cz cell B mostly conserves the regeneration-induced gain established on cell level compared to the FZ reference cell during TC. Cz cell A is partly regenerated during TC95 with simultaneous current injection and is not completely re-degraded again upon TC200 testing. The data could be interpreted to indicate a slight destabilization of the regenerated state in both Cz cells during TC200 testing without current injection. However, this interpretation has to be further investigated on a broader statistical basis.

3.3. Damp heat

Using the same extrapolation of Herguth's data for the destabilization of the regenerated state as during the TC200 test and assuming a temperature of 85 °C in the dark as applied during damp-heat testing, the regeneration-induced V_{oc} gain is expected to reduce to $V_{oc,gain}(500\ \text{h}) \approx 57\%$ and $V_{oc,gain}(1500\ \text{h}) \approx 19\%$ of its value prior to damp-heat testing. Taking into account the theoretically expected additional 10% loss during TC200, $V_{oc,Cz}(500/1500\ \text{h}) = 641/638$ mV would be expected for both Cz cells. Hence, in contrast to the expected $\Delta V_{oc} \approx 1$ mV for TC200 which is difficult to verify experimentally, an effect in the order of $\Delta V_{oc} \approx 4/7$ mV is more likely to be detectable even with the limited number of investigated samples. Measured values are $V_{oc,Cz\ A/B}(\text{DH500}) \approx 643/644$ mV and $V_{oc,Cz\ A/B}(\text{DH1000}) \approx 638/639$ mV after DH500 and DH1000 and subsequent illumination, respectively. Hence, the agreement, on a first view, seems rather good, especially after DH1000. However, considering *pFF*, 50% of the regeneration-induced gain for Cz cell A and 80% for Cz cell B are sustained during damp-heat testing. For a conclusive interpretation of the data, it needs to be considered that V_{oc} of the FZ reference cell decreases by about 4 mV in-between DH500 and DH1000 which is not linked to the BO defect. When comparing the values after DH500 and the subsequent illumination step, values of $\Delta V_{oc} = -3$ mV and $\Delta pFF = -0.6/-0.4\%_{abs}$ result for Cz cells A/B compared to the FZ reference cell whose values are stable. For DH1000 and its subsequent illumination step, values of $\Delta V_{oc} = -4/-2$ mV and $\Delta pFF = -0.7/-0.5\%_{abs}$ result for Cz cells A/B compared to the FZ reference cell whose values are again stable.

For a more meaningful interpretation of the defect states during damp-heat testing, ΔV_{oc} for varying illumination level compared to the annealed state is considered, see Fig. 4c. After DH500, the injection dependence of Cz cell A is less pronounced than before, compare Fig. 4b. This indicates partial annealing of the BO defect. Upon subsequent illumination, the injection dependence of ΔV_{oc} is significantly more pronounced with an illumination-induced difference of $\Delta V_{oc}(E=0.05\ \text{suns}) = -6$ mV at the pMPP compared to the already discussed $\Delta V_{oc}(E=1.0\ \text{sun}) = -3$ mV. Also, the shape of ΔV_{oc} approaches the shape of Cz cell A being in the degraded state, compare Fig. 4a. For Cz cell B, illumination-induced differences after DH500 of $\Delta V_{oc}(E=0.05\ \text{suns}) = -5$ mV and $\Delta V_{oc}(E=1.0\ \text{sun}) = -3$ mV result, also indicating a slightly more pronounced injection dependence upon illumination. However, the shape of ΔV_{oc} does not fully exhibit the characteristic kink as in the degraded state.

Right after DH1000 all three cells exhibit a similar increase in ΔV_{oc} compared to the values after DH500 across the considered injection range, see Fig. 4c. For all cells, ΔV_{oc} is almost independent of injection level indicating again partial annealing of the BO defect. Since ΔV_{oc} shifts homogeneously across the entire injection range, the observed V_{oc} loss is suspected to be process-induced by DH1000 which is also indicated by the FZ cell. Upon subsequent illumination, ΔV_{oc} of the FZ cell does not change significantly while for the Cz cells a stronger injection dependence results. Especially for Cz cell A, the ΔV_{oc} characteristic approaches the shape of the cell being in the degraded state. Illumination-induced changes after DH1000 are $\Delta V_{oc}(E=0.05\ \text{suns}) = -8$ mV and $\Delta V_{oc}(E=1.0\ \text{sun}) = -4$ mV for Cz cell A and $\Delta V_{oc}(E=0.05\ \text{suns}) = -5$ mV and $\Delta V_{oc}(E=1.0\ \text{sun}) = -3$ mV for Cz cell B. The larger difference between Cz cells A and B could be explained by Cz cell A being only partially regenerated during TC95. This would cause a higher percentage of the BO defect being in the degraded state after the same temperature treatment as for Cz cell B. Since right after DH, also the non-regenerated part of the BO defect seems to be in the annealed state which is then transformed into the degraded state during subsequent illumination, the described losses cannot be added. When taking into account the process-induced degradation of the FZ reference cell during DH1000, Cz cells A/B degrade by $\Delta V_{oc} = -2/-3$ mV and $\Delta pFF = -0.5/-0.4\%_{abs}$ compared to the values after regeneration on module/cell level over the entire experiment. The regeneration gain compared to the FZ reference was $\Delta V_{oc} = 7/8$ mV and $\Delta pFF = 0.5/1.1\%_{abs}$. That is, a value of $V_{oc,gain} \approx 78/68\%$ remains after testing which is significantly higher than the value of 19% given above from extrapolated literature data. Although it is not possible to completely clarify if the V_{oc} of the Cz cells exhibits the same amount of process-induced degradation as the FZ reference during DH1000, the higher change in injection dependence upon illumination after DH testing indicates a higher amount of destabilization with increasing time.

When considering the treatment-induced changes across the entire experiment, a regeneration-induced gain in V_{oc} and *pFF* can be conserved, see Fig. 3c. If taking into account the process-induced deterioration of the FZ reference cell during DH1000, see Fig. 3d, an even higher amount of the regeneration-induced gain can be conserved. Due to the change of the reference cell

during DH1000 quantitative statements are difficult. However, it can be stated that the conserved regeneration-induced gain probably lies within the range of 25% to 70%. This is supported by 50% of the regeneration-induced gain in *pFF* being conserved during testing, at least for Cz cell B. The discussed findings are valid for the industrial Cz silicon wafers used with a base resistivity of $\rho_{b,Cz}=2.3\ \Omega$ cm. The kinetics of the BO defect formation and reformation processes are expected to be different for varying material parameters such as boron and oxygen concentration. This will directly affect the quantitative impact on cell/module parameters such as V_{oc} for the discussed time regimes of thermal cycling and damp-heat testing. However, the qualitative findings of (partial) regeneration during TC with current injection and (partial) destabilization during damp-heat testing are expected to also be valid for Cz silicon wafers with differing boron and oxygen concentrations.

4. Summary and conclusion

It has been shown that the regenerated state is almost completely stable upon thermal cycling and that regeneration of the BO complex can even occur during module certification when current is injected during the treatment. This applies, for example, during the "TC200 test" within certification standard IEC-61215. During long times of damp-heat testing, our data indicate a reduction of the regeneration-induced gain while it does not vanish completely. More than half the gain in *pFF* is maintained on a cell being conditioned in the regenerated state prior to module assembly which supports the conclusion that the BO complex has not re-formed completely.

Since during module certification, the maximum output power is measured to evaluate the influence of different certification steps, care should be taken even if the modules are in the degraded state before the start of certification testing. Certification testing could be optimized to take possible regeneration and annealing effects of the BO defect during different certification steps into account.

More long-term testing of regenerated solar cells under accelerated aging conditions is needed to support the findings of this paper on a broader statistical basis.

As already mentioned by Herguth [9] and confirmed within this paper in section 3, regeneration already occurs at comparably low temperatures such as 85 °C (and below) and simultaneous carrier injection, which are conditions that can be reached within solar modules exposed to sunlight and operated in (or close to) open circuit conditions. This implies that the maximum power output of photovoltaic systems might be sustainably increased by keeping the system in (or close to) open circuit conditions while being exposed to sunlight (for example during installation when all modules are still in open circuit).

Acknowledgements

The authors acknowledge U. Jäger for allocation of the investigated solar cells, M. Tranitz for module manufacturing, F. Schwehr for *I–V* measurements, Fraunhofer ISE TestLab PV Modules for certification testing and J. Greulich for fruitful discussions. Part of this work was supported by the German Federal Ministry of Environment, Nature Conservation and Nuclear Safety under Contract No. 0329849B (MASSE).

References

[1] W. Zulehner, D. Huber, Crystal Growth, Properties and Applications, Springer Verlag, 1982.
[2] A. Goetzberger, J. Knobloch, B. Voss, Crystalline Silicon Solar Cells, John Wiley & Sons Ltd, Chichester, UK, 1998.
[3] J. Schmidt, K. Bothe, Structure and transformation of the metastable boron- and oxygen-related defect center in crystalline silicon, Phys. Rev. B: Condens. Matter 69 (2004) 0241071–0241078.
[4] V.V. Voronkov, R. Falster, Latent complexes of interstitial boron and oxygen dimers as a reason for degradation of silicon-based solar cells, J. Appl. Phys. 107 (2010) 1–8.
[5] S. Rein, W. Warta, S.W. Glunz, Investigation of carrier lifetime in p-type Cz–silicon: specific limitations and realistic prediction of cell performance, in: Proceedings of the 28th IEEE Photovoltaics Specialists Conference, Anchorage, Alaska, USA, 2000, pp. 57–60.
[6] J. Schmidt, B. Lim, D. Walter, K. Bother, S. Gatz, T. Dullweber, P.P. Altermatt, Impurity-related limitations of next-generation industrial silicon solar cells, IEEE J. Photovoltaics 7 (2013) 114–118.
[7] S.W. Glunz, S. Rein, W. Warta, J. Knobloch, W. Wettling, On the degradation of Cz-silicon solar cells, in: Proceedings of the Second World Conference on Photovoltaic Energy Conversion, Vienna, Austria, 1998, pp. 1343–1346.
[8] J. Schmidt, A.G. Aberle, R. Hezel, Investigation of carrier lifetime instabilities in Cz-grown silicon, in: Proceedings of the 26th IEEE Photovoltaic Specialists Conference, Anaheim, California, USA, 1997, pp. 13–18.
[9] A. Herguth, G. Schubert, M. Kaes, G. Hahn, A new approach to prevent the negative impact of the metastable defect in boron doped cz silicon solar cells, in: Proceedings of the Fourth World Conference on Photovoltaic Energy Conversion, Waikoloa, Hawaii, USA, 2006, pp. 940–943.
[10] B. Lim, Boron–Oxygen-Related Recombination Centers in Crystalline Silicon and the Effects of Dopant-Compensation, Thesis, Fakultät für Mathematik und Physik, Universität Hannover, Hannover, 2012.
[11] A. Herguth, G. Hahn, Boron–oxygen related defects in Cz–silicon solar cells degradation, regeneration and beyond, in: Proceedings of the 24th European Photovoltaic Solar Energy Conference, Hamburg, Germany, 2009, pp. 974–976.
[12] F. Fertig, J. Greulich, J. Broisch, D. Biro, S. Rein, Stability of the regeneration of the boron-oxygen complex in silicon solar cells during module integration, Sol. Energy Mater. Sol. Cells 115 (2013) 189–198.
[13] IEC-61215, Crystalline silicon terrestrial photovoltaic (PV) modules—Design qualification and type approval, 2nd ed., International Electrotechnical Commission, 2005.
[14] UL-1703, Flate-Plate Photovoltaic Modules and Panels, 3rd ed., Underwriters Laboratories Inc., 2002.
[15] A.W. Blakers, A. Wang, A.M. Milne, J. Zhao, M.A. Green, 22.8% efficient silicon solar cell, Appl. Phys. Lett. 55 (1989) 1363–1365.
[16] D. Biro, R. Preu, S.W. Glunz, S. Rein, J. Rentsch, G. Emanuel, I. Brucker, T. Faasch, C. Faller, G. Willeke, J. Luther, PV-Tec: Photovoltaic technology evaluation center—design and implementation of a production research unit, in: Proceedings of the 21st European Photovoltaic Solar Energy Conference, Dresden, Germany, 2006, pp. 621–624.
[17] E. Schneiderlöchner, R. Preu, R. Lüdemann, S.W. Glunz, Laser-fired rear contacts for crystalline silicon solar cells, Prog. Photovoltaics Res. Appl. 10 (2002) 29–34.
[18] S. Mack, U. Jäger, G. Kästner, E.A. Wotke, U. Belledin, A. Wolf, R. Preu, D. Biro, Towards 19% efficient industrial PERC devices using simultaneous front emitter and rear surface passivation by thermal oxidation, in: Proceedings of the 35th IEEE Photovoltaic Specialists Conference, Honolulu, Hawaii, USA, 2010, pp. 17–21.
[19] U. Jäger, S. Mack, C. Wufka, A. Wolf, D. Biro, R. Preu, Benefit of selective emitters for p-type silicon solar cells with passivated surfaces, IEEE J. Photovoltaics 3 (2013) 621–627.
[20] R.A. Sinton, A. Cuevas, A quasi-steady-state open-circuit voltage method for solar cell characterization, in: Proceedings of the 16th European Photovoltaic Solar Energy Conference, Glasgow, UK, 2000, pp. 1152–1155.
[21] J. Schmidt, A. Cuevas, S. Rein, S.W. Glunz, Impact of light-induced recombination centres on the current-voltage characteristic of Czochralski silicon solar cells, Prog. Photovoltaics Res. Appl. 9 (2001) 249–255.
[22] A. Herguth, G. Schubert, M. Kaes, G. Hahn, Avoiding boron–oxygen related degradation in highly boron doped cz silicon, in: Proceedings of the 21st European Photovoltaic Solar Energy Conference, Dresden, Germany, 2006, pp. 530–537.
[23] B. Lim, A. Liu, D. Macdonald, K. Bothe, J. Schmidt, Impact of dopant compensation on the deactivation of boron–oxygen recombination centers in crystalline silicon, Appl. Phys. Lett. 95 (2009) 1–3.
[24] A. Herguth, G. Schubert, M. Kaes, G. Hahn, Investigations on the long time behavior of the metastable boron–oxygen complex in crystalline silicon, Prog. Photovoltaics Res. Appl. 16 (2008) 135–140.
[25] M. Glatthaar, J. Haunschild, M. Kasemann, J. Giesecke, W. Warta, S. Rein, Spatially resolved determination of dark saturation current and series resistance of silicon solar cells, Phys. Status. Solidi. RRL 4 (2010) 13–15.
[26] M.A. Green, Solar cells: operating principles, Technol. Syst. Appl. (1986). (UNSW, Kensington).